2010 IEEE International Conference on Robotics and Automation
Anchorage Convention District
May 3-8, 2010, Anchorage, Alaska, USA

Central Catadioptric Line Matching for Robotic Applications

Pascal Vasseur
MIS - University of Picardie Jules Verne, Amiens, France
Heudiasyc - University of Technology of Compiègne, France
Email: Pascal.Vasseur@u-picardie.fr

Cédric Demonceaux
MIS - University of Picardie Jules Verne
Amiens, France
Email: Cedric.Demonceaux@u-picardie.fr

***Abstract*—This paper presents a method for catadioptric line matching across multiple images. While most of previous works deals with vertical lines and planar motion, our approach is able to match any kind of lines between two views separated by a rigid transformation without any prior knowledge of the epipolar geometry. Catadioptric lines are represented by their normals in sphere space and we use only these normals and their relative positions in order to perform the matching. A geometric hashing approach allows in the first image to construct hashing tables based on bases defined by every possible couples of normals. In the second image, a voting scheme permits to select the best corresponding bases and subsequently to match catadioptric lines. We show that the proposed representation is invariant in the case of a pure rotation and quasi-invariant for a combination of rotation and translation. We also propose different experimental results obtained in real time on real outdoor sequences.**

I. INTRODUCTION

Straight line segments are very useful features in computer vision and in robotic applications. They are particularly suitable for man made environments and allow to perform 3D reconstruction or motion estimation between three images [5] [15] or two images under some hypotheses [21] [34]. Line segments are generally less numerous than interest points but richer in information. Moreover, their detection is very reliable according to their orientation. Despite these advantages, line matching is a particularly difficult problem and only few works have been proposed in literature. These difficulties proceed from different reasons such as the inaccuracy of the endpoint extraction, the poor geometric disambiguity constrain and the lack of significant photometric information in the local neighborhood. Consequently, there is no real reference method as in the case of points, but we can separate line matching methods into two classes. The first class includes methods which perform the matching of each line separately [2] [23] [33] while the second corresponds to groups of line matching methods [22] [18] [13].

Catadioptric sensors have taken for many years a growing importance in applications such as SLAM (Simultaneous Localization And Mapping) [19], 3D reconstruction [20], visual servoing [14], rotation estimation [10] [8] and we know that catadioptric lines have some interesting properties such as the projection of vanishing points in the image. In the case of catadioptric images, 3D straight lines are projected into conics. Consequently, the majority of catadioptric line matching methods deals only with 3D lines parallel to the optical axis [9] [17] [25] [26] [27] [31]. Indeed, in this case conics are degenerated into radial lines. Similarly than the perspective case, catadioptric line matching methods are also divided in two classes respectively based on a separate matching [26] [27] and on group matching [9].

In the case of individual matching, geometric attributes of the lines such as length, orientation, overlapping were first used [1] [2] [23]. These methods are based on the prediction-verification techniques which consist in assuming some initial matchings and in growing the set of matchings. The inital matchings are generally based on local properties while the verification is based on more global constrains. More recently, some works have been done in order to develop stable descriptors which can described efficiently line segments between different perspective views [12] [30] or catadioptric views [26] [27]. However, most of these methods [12] [26] [27] deal with vertical lines only. Due to the distorsions of the catadioptric images, this kind of methods based on descriptors, correlation or geometric attributes are particularly inefficient in the case of general lines.

Matching groups of lines allows to benefit from the supplementary geometric information provided by their spatial relationships [22] [18] [13]. However, these approaches are very sensitive to the quality of detection. Other methods such as [16] and [28] consider the epipolar geometry as known and can then constrain the search space. In our case, the epipolar geometry is not a priori known.

The work presented in this paper belongs to the group of line matching category. We propose an invariant or quasi-invariant representation of line groups if the motion is respectively a rotation or a rigid transformation. We develop an adaptation of the geometric hashing [18] applied to the first image in order to build different indexing tables. Geometric hashing consists in using some detected features as a frame in order to express the other feature coordinates. In our case, the features correspond to normals of great circles in the sphere space which are the projections of 3D lines. Two normals are then sufficient to form a basis and to compute the spherical coordinates of the other normals. These spherical coordinates are integrated in an hashing table in order to provide a signature of the basis. Each couple of normals is then represented by an hashing table. The second

step is based on the peaking effect proposed in [7] which describes the probability distributions of angles and length ratios of two segments from random viewing directions. We adapt this effect to the angle between normals of great circles and use this phenomenon in the second image. The aim is to find iteratively a pair of normals in the second image which verifies the peak effect according to an other pair of the first image. A voting method based on the hashing tables is then used in order to verify the peaking effect. Once a pair of bases has been matched between the two frames, the other lines can be matched directly by a simple verification.

The main contributions of our method are the following :

- The method is not restricted to vertical lines and can treat any oriented lines.
- The invariant or quasi-invariant representation allows to support respectively rotations and rigid transformations between the views. The quality of the matching is then only bounded by the ratio between baseline and scene depth. We show that the performances of the method decrease slowly according to the length of the baseline.
- No prior knowledge about the epipolar geometry is required. Only the intrinsic parameters are necessary in order to compute the equivalent spherical image.
- The method is robust to luminance changes since we use only geometric information.
- The method is very fast and proposes a real time line matching.

The main limit of the method is the length of the baseline according to the mean distance between the camera and the 3D lines. For a baseline with a length less than 30% of this mean distance, the rate of correct matching between two images is approximately equal to 85%. The performances decrease severely beyond this limit. The second limitation is the single viewpoint requirement of the sensor.

The rest of the paper is organized as follows. Section 2 is dedicated to the central catadioptric lines and their properties during a camera motion. We present in Section 3 the construction of indexing tables while Section 4 proposes our voting method and the final matching. We show experimental results on real sequences in Section 5 before a conclusion.

II. CENTRAL CATADIOPTRIC LINES AND THEIR PROPERTIES

A. Catadioptric Line Formation and Detection

It has been proven that central catadioptric sensors with a single point of view [3] can be represented by two projections via a unitary sphere [11]. Consequently, 3D lines are projected on the sphere as great circles and in the image plane as conics [4]. In this way, catadioptric lines can be represented by the normal of their equivalent great circle on the sphere if the intrinsic parameters of the sensor are known. Besides, most of the catadioptric line detection methods assume the knowledge of the intrinsic parameters [6] [24] [29] [32]. In our case, we use the adaptation of the polygonal approximation described in [6] for our line detection. In the rest of the paper, we then consider that a catadioptric line corresponds to a normal on the unitary sphere.

B. Catadioptric Lines in Motion

This part deals with the behaviour of different normals when the catadioptric sensor is in motion and analyzes their relative spatial relations. In this way, we consider p lines in the first image I_1 and q lines in I_2. We assume the motion between I_1 and I_2 to be a rigid transformation (rotation R and translation t).

Let n_i with $i = 1 \dots p$ be the normals of p lines (great circles) in I_1 and $n_j^{'}$ with $j = 1 \dots q$ the normals of q lines (great circles) in I_2.

Property

If i and j are matched $n_i \leftrightarrow n_j^{'}$, then $n_j^{'} \sim Rn_i + t \times Ru$ where u is the direction of the corresponding 3D line.

1) Catadioptric Lines in Motion with Pure Rotation: If $t = 0$, $n_j^{'} = Rn_i$. Thus, if i_1 and i_2 are respectively matched with j_1 and j_2, we have

$$n_{j_1}^{'} \cdot n_{j_2}^{'} = Rn_{i_1} \cdot Rn_{i_2} = n_{i_1} \cdot n_{i_2} \tag{1}$$

Proposition: A set of two matched lines is sufficient to determine the other matching.

Hypothesis: $n_1 \leftrightarrow n_1^{'}$
$n_2 \leftrightarrow n_2^{'}$ (after rearrangement of vectors)

Let note $\mathcal{N}_1 = \{n_i, i = 1 \dots p\}$ the normal family in I_1 and $\mathcal{N}_2 = \{n_j^{'}, j = 1 \dots q\}$ the normal family in I_2. We assume two normals n_1 and n_2 in I_1 such as $n_1 \times n_2 \neq 0$. Let pose $n_3 = n_1 \times (n_1 \times n_2)$. Then, $\{n_1, n_3, n_1 \times n_3\}$ is an orthonormal basis of $\mathcal{N}_1$.
In this way, we have

$$\forall i = 1 \dots p, n_i = (n_i \cdot n_1)n_1 + (n_i \cdot n_3)n_3 + (n_i \cdot (n_1 \times n_3))n_1 \times n_3 \tag{2}$$

Similarly :

$$\forall j = 1 \dots q, n_i^{'} = (n_i^{'} \cdot n_1^{'})n_1^{'} + (n_i^{'} \cdot n_3^{'})n_3^{'} + (n_i^{'} \cdot (n_1^{'} \times n_3^{'}))n_1^{'} \times n_3^{'} \tag{3}$$

Remark: Since $\|n_i\| = \|n_j^{'}\| = 1$, we can express 2 and 3 in spherical coordinates. In $\{n_1, n_3, n_1 \times n_3\}$, n_i has the following coordinates (θ_i, φ_i), where

$$\varphi_i = \arccos(n_i \cdot (n_1 \times n_3))$$

$$\theta_i = \begin{cases} \arccos \frac{n_i \cdot n_1}{\sqrt{(n_i \cdot n_1)^2 + (n_i \cdot n_3)^2}} \text{if } n_i \cdot n_3 \geq 0 \\ 2\pi - \arccos \frac{n_i \cdot n_1}{\sqrt{(n_i \cdot n_1)^2 + (n_i \cdot n_3)^2}} \text{if } n_i \cdot n_3 < 0 \end{cases}$$

Property: If $n_i \leftrightarrow n_j^{'}$ then $\theta_i = \theta_j^{'}$ and $\varphi_i = \varphi_j^{'}$. Thus, n_i and $n_j^{'}$ have similar coordinates in their own basis.

Proof: $n_i \cdot n_1 = n_j^{'} \cdot n_1^{'}$ (see 1)
$n_i \cdot n_2 = n_j^{'} \cdot n_2^{'}$

$$\begin{aligned} n_i \cdot n_3 &= n_i \cdot [(n_1 \cdot n_2)n_1 - n_2] \\ &= (n_1 \cdot n_2)(n_i \cdot n_1) - n_i \cdot n_2 \\ &= (n_1^{'} \cdot n_2^{'})(n_j^{'} \cdot n_1^{'}) - n_j^{'} \cdot n_2^{'} \\ &= n_j^{'} \cdot n_3^{'} \\ \theta_i &= \theta_j^{'} \end{aligned}$$

$$\begin{aligned} n_i \cdot (n_1 \times n_3) &= n_i \cdot [n_1 \times ((n_1 \cdot n_2)n_1 - n_2)] \\ &= -n_i \cdot (n_1 \times n_2) \end{aligned}$$

However, $\|n_1 \times n_2\| = |\sin(n_1 \cdot n_2)| = |\sin(n_1^{'} \cdot n_2^{'})| = \|n_1^{'} \times n_2^{'}\|$, then

$$\begin{aligned} n_i \cdot (n_1 \times n_3) &= n_j \cdot (n_1^{'} \times n_3^{'}) \\ \varphi_i &= \varphi_j^{'} \end{aligned}$$

Consequently, if we know two matched lines between I_1 and I_2, the other matchings can be deduced by the comparison of their spherical coordinates.

In order to find the initial set of two matched lines, we propose a voting method approach. Consider the following function :

$$\delta_{i,j,i^{'},j^{'}}(n,n^{'}) = \begin{cases} 1 \text{ if } |\theta_{i,j}^{n} - \theta_{i^{'},j^{'}}^{n^{'}}| < \epsilon_\theta \text{ and } |\varphi_{i,j}^{n} - \varphi_{i^{'},j^{'}}^{n^{'}}| < \epsilon_\varphi \\ 0 \text{ else} \end{cases} \tag{4}$$

Then, $\delta_{i,j,i^{'},j^{'}}(n,n^{'}) = 1$ if n and $n^{'}$ have the same spherical coordinates up to respectively ϵ_θ and ϵ_φ in their respective bases $\{n_i, n_i \times (n_i \times n_j), n_i \times n_j\}$ and $\{n_i^{'}, n_i^{'} \times (n_i^{'} \times n_j^{'}), n_i^{'} \times n_j^{'}\}$. We have then to find :

$$i,j,i^{'},j^{'} \,/\, \arg\max_{i,j,i^{'},j^{'}} \sum_{n=n_1}^{n_p} \sum_{n^{'}=n_1^{'}}^{n_q^{'}} \delta_{i,j,i^{'},j^{'}}(n,n^{'}). \tag{5}$$

2) Catadioptric Lines in Motion Including Translation: In this part, we aim at quantifying the influence of the translation on the angle between normals since there is no more invariance. This study is made according to the 3D line directions, the orthogonal distance between 3D lines and the camera center and the translation (we neglect the possible rotation since we have demonstrated the invariance previously).

Then, for two distinct 3D lines, we have :

$$\begin{aligned} s_1^{'} n_1^{'} &= s_1 n_1 + t \times u_1 \\ s_2^{'} n_2^{'} &= s_2 n_2 + t \times u_2 \end{aligned}$$

where s_i and $s_i^{'}$ are scale factors. The normalized dot product between $n_1^{'}$ and $n_2^{'}$ is equal to :

$$\begin{aligned} n_1^{'} \cdot n_2^{'} &= \frac{s_1^{'} n_1^{'} \cdot s_2^{'} n_2^{'}}{\|s_1^{'} n_1^{'}\| \|s_2^{'} n_2^{'}\|} \\ &= \frac{(s_1 n_1 + t \times u_1) \cdot (s_2 n_2 + t \times u_2)}{\|s_1 n_1 + t \times u_1\| \|s_2 n_2 + t \times u_2\|} \end{aligned}$$

If we decompose t such as $t = \alpha_1 u_1 + \beta_1 n_1 + \gamma_1 n_1 \times u_1$, we obtain :

$$\begin{aligned} s_1 n_1 + t \times u_1 &= s_1 n_1 + \beta_1 (n_1 \times u_1) + \gamma_1 (n_1 \times u_1) \times u_1 \\ &= n_1(s_1 - \gamma_1) + \beta_1 (n_1 \times u_1) \end{aligned}$$

and

$$\|s_1 n_1 + t \times u_1\|^2 = (s_1 - \gamma_1)^2 + \beta_1^2$$

Similarly, if we consider $t = \alpha_2 u_2 + \beta_2 n_2 + \gamma_2 (n_2 \times u_2)$, we obtain :

$$s_2 n_2 + t \times u_2 = n_2(s_2 - \gamma_2) + \beta_2 (n_2 \times u_2)$$

and

$$\|s_2 n_2 + t \times u_2\|^2 = (s_2 - \gamma_2)^2 + \beta_2^2$$

Dot product is then equal to :

$$n_1^{'} \cdot n_2^{'} = \frac{[n_1(s_1 - \gamma_1) + \beta_1 (n_1 \times u_1)] \cdot [n_2(s_2 - \gamma_2) + \beta_2 (n_2 \times u_2)]}{\sqrt{((s_1 - \gamma_1)^2 + \beta_1^2)((s_2 - \gamma_2)^2 + \beta_2^2)}}$$

The behaviour of the normals depend then on the ratio between s_1, s_2 related to the scene depth and $\beta_1, \beta_2, \gamma_1, \gamma_2$ related to the translation magnitude and orientation. For example, if we consider that the scene depth is largely more important than the magnitude of the translation, i.e. $s_1 \gg \gamma_1, s_2 \gg \gamma_2, s_1 \gg \beta_1, s_2 \gg \beta_2$, then the dot product becomes :

$$n_1^{'} \cdot n_2^{'} \simeq n_1 \cdot n_2 + \epsilon, \text{ where } \epsilon \simeq 0$$

We have estimated the angle difference between two normals for 100000 simulations of any couple of 3D lines with any possible translation (Figure 1). We can see that even for a translation equal to the scene depth, the angle difference between the normals in consecutive images is less than 20 degrees. Consequently, we propose to use the same voting approach than in the pure rotation case in order to find the initial set of two matched normals. The next parts are dedicated to the implementation details of the algorithm.

III. HASHING TABLE CONSTRUCTION

Since we have demonstrated that knowing two matched lines, we can deduce the other matchings, we propose to use a geometric hashing algorithm [18] in order to find this set of two initial matched normals. Geometric hashing consists in selecting a set of features as basis and in expressing the coordinates of the other features in this basis. In our case, we know that we can form a basis from two normals. In this way, if we consider every possible set of two normals in the first image, the aim will consist in finding in the next image a set of two normals corresponding to one of these basis in

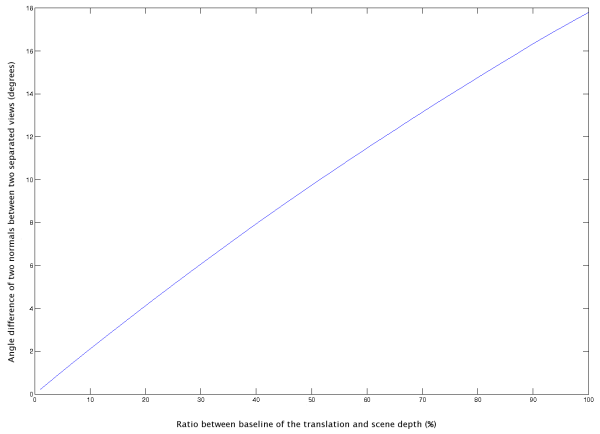

Fig. 1. Angle difference between two normals in consecutive views for 100000 trials.

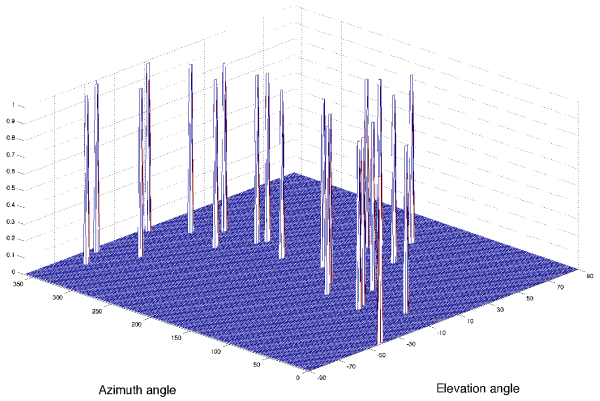

Fig. 2. Example of an hashing table associated to a couple of normals. 10 other normals consitute the descriptor.

the first image. The hashing table is then the first step for the characteristic function proposed in equation 4.

Rather than exploring every couple of normals in the first image, we propose to select p normals associated to the longest lines (the length is equivalent to the number of pixels) in order to maximize the probability to find the same lines in the next image. Among these p normals, we then consider every combination of two normals to form different bases. For each basis, we define a descriptor composed by the spherical coordinates $(\theta^n_{i,j}, \varphi^n_{i,j})$ of the $p-2$ remaining normals. It is worth noting that for each great circle, we consider its two antipodal normals since it is impossible to disambiguate them after a motion.

Each basis is then represented by a hashing table. The axes of such a table correspond to the spherical coordinates in the interval $[0; 2\pi[$ and $\left[-\frac{\pi}{2}; \frac{\pi}{2}\right]$. The values of the hashing table are binary. 1 corresponds to the presence of a normal n and is applied to its neighborhood defined by parameters ϵ_θ and ϵ_φ as described in equation 4. Figure 3 illustrates a hashing table associated to a couple of normals and described by 10 other normals.

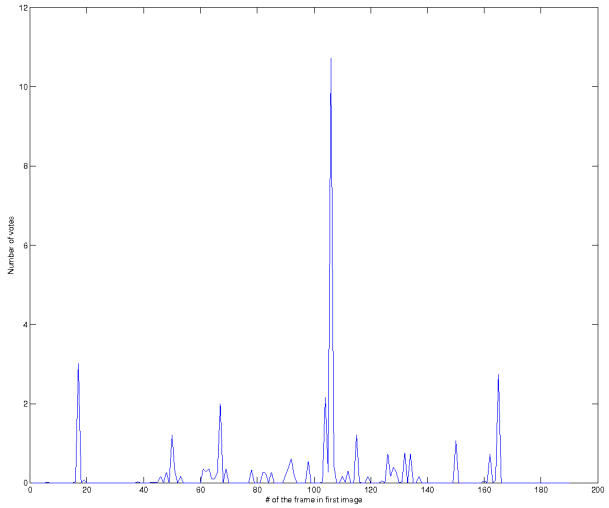

Fig. 3. Example of voting for a couple of normals in the second image according to all the frames in the first image.

IV. MATCHING

The matching is divided into two steps which are respectively the initial basis matching by voting followed a verification step. The voting part aims at solving equation 5 by searching a basis of two normals in the second image which corresponds to one of the bases proposed in the first image. The verification step consists in matching the other normals.

A. Basis Matching by Voting

The method consists in considering the two longest catadioptric lines and their normals $i^{'}, j^{'}$ as a potential basis. We choose the longest lines in order to maximise the probability to select a frame already referenced in the first image. Similarly than previously, we express the spherical coordinates of the q other normals according to the basis $i^{'}, j^{'}$. We then apply the equation 4 by accumulating the votes for each basis of the first image. Figure 3 shows an example of voting for a couple of normals in the second image according to whole possibilities of frames among ten normals in the first image. We can note that an individual peak of votes appears at the 106^{th} frame of the first image. If there is no detected peak, we consider an other couple of normals in order to find an initial basis matching.

B. Verification and Final Matching

The verification step consists in counting the total number of normal matchings obtained from the bases selected in the previous step. In this way, the spherical coordinates of the normals detected in both images are expressed in their respective bases i, j and $i^{'}, j^{'}$. Two normals are then matched if their spherical coordinates verify the conditions of the equation 4. In order to avoid multiple matchings, we apply a cross-verification. Indeed, we associate the closest normals which verify equation 4 respectively between the first and second images and between the second and first images. If we

obtain the same couple of normals, the matching is validate otherwise it is cancelled. If the number of total matched normals is at least equal to the half of the number of normals, the final matching is accepted. At the contrary, if the number of matching is insufficient the voting step is repeated with an other couple of normals.

V. EXPERIMENTAL RESULTS

A. Introduction

Results are given for two different outdoor sequences acquired with a paracatadioptric sensor of RemoteReality company. Each sequence represents a distance around fifty meters and is submitted to several changes of environment and luminance conditions. The first sequence has been captured continuously during the motion (small baseline) while the second is constituted by images taken every meter (wide baseline). In both sequences, the mean number of detected lines is equal to 40. In order to evaluate the performances of the method, we propose different measures such as the percentage of total good matching (TGM), the mean number of consecutive line matching (CLM) and the percentage of good matching per image (GMI). TGM represents the ratio between the number of consecutive pair of views correctly matched and the number of pair of images in the sequence. CLM describes the capacity to track a particular line consecutively, it is equal to the mean number of consecutive matchings in the sequence. GMI corresponds to the number of line matchings according to the number of possible line matchings.

B. Sequence with Small Baseline

Figure 4 proposes the matching result for two consecutive views with a small baseline. The lines with similar colors are matched. A part of the sequence can be viewed in supplementary material. Figure 4 illustrates perfectly a successful matching between two views. TGM is equal to 96%, which means that the matching is almost perfect during this sequence. CLM is equal to 9.5 with several peaks between 60 and 65. We are then able to track some lines during 65 consecutive images and almost 10 in the general case. GMI is around 88% but can reach 100% for some couple of images. During the sequence, we have also noted that even in the case of blurry images, the method is able to detect most of the lines and to match them correctly (see supplementary material). It is worth noting that in all experiments, we fixed $p = 10$.

In order to test deeply the approach by increasing the baseline, we also applied the matching every five images. In this case, we obtain TGM equal to 84%. However, we do not have precisely the real baseline and can not judge the significance of this result. CLM is slightly greater than 4 with a maximum of 38. GMI is equal to 69% due to the variation of the detected lines essentially on the surrounding of the images (see supplementary material).

C. Sequence with Large Baseline

Figure 5 shows an example of the results obtained with our method for a baseline equal to one meter. The sequence contains 90 images and we obtain TGM, CLM and GMI respectively equal to 82.5%, 6.5 and 80%. These results demonstrate the validity of the method even in presence of large motions. Figure 6 presents results obtained for a baseline equal to 3 meters. It is worth noting that in all the experiments, we always use the same ϵ_θ and ϵ_φ both equal to 3 degrees.

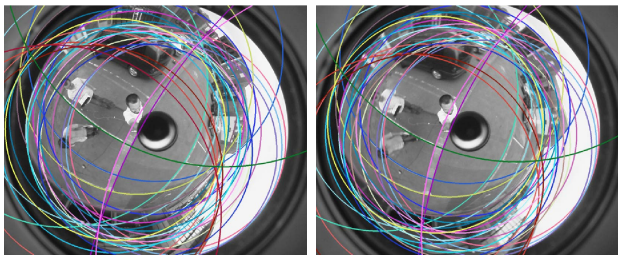

(a) (b)

Fig. 4. Two consecutive images with small baseline. Lines with similar color are matched.

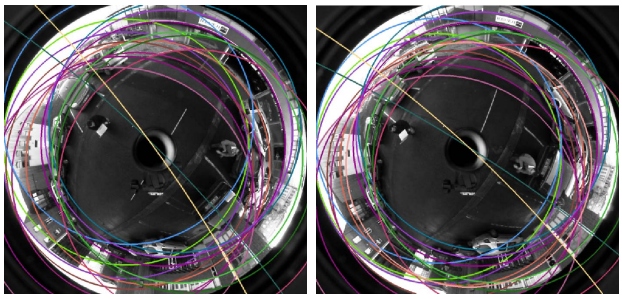

(a) (b)

Fig. 5. Two consecutive images with large baseline. Lines with similar color are matched.

VI. CONCLUSION

In this paper, we proposed a method for catadioptric line matching based on an invariant or quasi-invariant representation of line groups according to respectively rotation or rigid transformation between views. We proposed an adaptation of geometric hashing and peak effect in order to perform this line matching. This method presents several advantages :

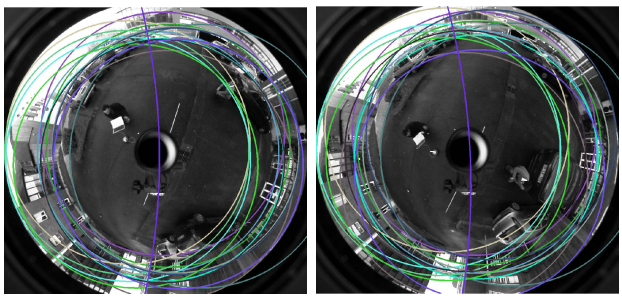

(a) (b)

Fig. 6. Two images with a baseline of 3 meters. Lines with similar color are matched.

- It is very fast, each pair of views is treated in less than 10 ms.
- There is no restriction about the 3D line orientation.
- 3D motions are allowed between views as well as large baselines.
- It is robust to luminance variations.

Future works will consist in using the results of the method for 3D reconstruction and motion estimation. We also aim at extending the method for the line matching between heterogeneous central vision sensors (catadioptric, perspective, fisheye). In this way, we will add some photogrammetric measures such as color histograms in order to robustify the matching.

ACKNOWLEDGMENT

This work was supported by the Région Picardie (ALTO Project) and also by the Programme Hubert Curien STAR (NOVA Project).

REFERENCES

[1] N. Ayache and B. Faverjon, "Efficient Registration of stereo images by matching graph descriptions of edge segments", In International Journal of Computer Vision (IJCV), Vol. 1, N2, pp. 107-131, 1987.

[2] N. Ayache, "Artificial Vision for Mobile robots - Stereo-vision and Multisensor Perception", MIT-Press, 1991.

[3] S. Baker and S.K. Nayar, "A Theory of Single-Viewpoint Catadioptric Image Formation", In International Journal of Computer Vision (IJCV), Vol. 35, N2, pp. 175-196, 1999.

[4] J.P. Barreto and H. Araujo, "Geometric Properties of Central Catadioptric Line Images", In Proc. European Conference on Computer Vision (ECCV02), Copenhagen, Denmark, pp. 237-251, 2002.

[5] A. Bartoli and P. Sturm, "Structure-from-motion using lines: Representation, triangulation, and bundle adjustment", In Computer Vision and Image Understanding (CVIU), Vol. 100, N3, pp. 416-441, 2005.

[6] J. C. Bazin, C. Demonceaux and P. Vasseur, "Fast Central Catadioptric Line Extraction", In Proc. Iberian Conference on Pattern Recognition and Image Analysis (IbPRIA07), Girona, Spain, pp. 25-32, 2007.

[7] J. Ben-Arie, "The probabilistic peaking effect of viewed angles and distances with application to 3D object recognition", In IEEE Trans. on Pattern Analysis and Machine Intelligence (PAMI), Vol. 12, N8, pp. 760-774, 1990.

[8] M. Bosse, R.J. Rikoski, J.J. Leonard and S.J. Teller, "Vanishing points and three-dimensional lines from omni-directional video", In The Visual Computer, Vol. 19, N6, pp. 417-430, 2003.

[9] E. Brassart, L. Delahoche, C. Cauchois, C. Drocourt, C. Pegard and E.M. Mouaddib, "Experimental Results got with the Omnidirectional Vision Sensor SYCLOP", In Proc IEEE Workshop on Omnidirectional Vision (OMNIVIS00), Hilton Head Island, SC, USA, pp. -, 2000.

[10] C. Demonceaux, P. Vasseur and C. Pégard, "UAV Attitude Computation by Omnidirectional Vision in Urban Environment", In Proc. IEEE International Conference on Robotics and Automation (ICRA07), Roma, Italy, pp. 2017-2022, 2007.

[11] C. Geyer and K. Daniilidis, "Catadioptric Projective Geometry", In International Journal of Computer Vision (IJCV), Vol. 45, N3, pp. 223-243, 2001.

[12] T. Goedeme, T. Tuytelaars and L.J. Van Gool, "Fast wide baseline matching for visual navigation", In Proc. IEEE Computer Society Conference on Computer Vision and Pattern Recognition (CVPR04), Washington, DC, USA, pp. 24-29, 2004.

[13] P. Gros, O. Bournez and E. Boyer, "Using Local Planar Geometric Invariants To Match And Model Images Of Line Segments", In Computer Vision and Image Understanding (CVIU), Vol. 69, N2, pp. 135-155, 1998.

[14] H. Hadj-Abdelkader, Y. Mezouar, P. Martinet and F. Chaumette, "Catadioptric Visual Servoing From 3-D Straight Lines", In IEEE Trans. on Robotics (TRO), Vol. 24, N3, pp. 652-665, 2008.

[15] R.I. Hartley, "Projective Reconstruction and Invariants from Multiple Images", In IEEE Trans. on Pattern Analysis and Machine Intelligence (PAMI), Vol. 16, N10, pp. 1036-1041, 1994.

[16] R.I. Hartley, "A Linear Method For Reconstruction From Lines And Points", In Proc. International Conference on Computer Vision (ICCV95), Boston, MA, USA, pp. 882-887, 1995.

[17] S. Kim and S.Y. Oh, "SLAM in Indoor Environments using Omnidirectional Vertical and Horizontal Line Features", In Journal of Intelligent and Robotic Systems (JIRS), Vol. 51, N1, pp. 31-43, 2008.

[18] Y. Lamdan and H.J. Wolfson, "Geometric Hashing: A General And Efficient Model-Based Recognition Scheme", In Proc. International Conference on Computer Vision (ICCV88), Tampa, FL, USA, pp. 238-249, 1988.

[19] T. Lemaire and S. Lacroix, "SLAM with Panoramic Vision", In Journal of Field Robotics, Vol. 24, pp. 91-111, 2007.

[20] M. Lhuillier, "Automatic scene structure and camera motion using a catadioptric system",In Computer Vision and Image Understanding (CVIU), Vol. 109, N2, pp. 186-203, 2008.

[21] G. Lopez Nicolas, J.J. Guerrero, O.A. Pellejero and C. Sagues, "Computing Homographies from Three Lines or Points in an Image Pair", In Proc. International Conference on Image Analysis and Processing (ICIAP05), Cagliary, Italy, pp. 446-453, 2005.

[22] M.I.A. Lourakis, S.T. Halkidis and S.C. Orphanoudakis, "Matching disparate views of planar surfaces using projective invariants", In Image and Vision Computing (IVC), Vol. 18, N9, pp. 673-683, 2000.

[23] G. Medioni and R. Nevatia, "Segment-Based Stereo Matching", In Computer Vision, Graphics, and Image Processing, Vol. 31, N1, pp. 2-18, 1985.

[24] C. Mei and E. Malis, "Fast central catadioptric line extraction, estimation, tracking and structure from motion", In Proc. IEEE/RSJ International Conference on Intelligent Robots and Systems (IROS06), Beijing, China, pp. 4774-4779, 2006.

[25] D. Prasser, G. Wyeth, M. Milford, J. Roberts and K. Usher, "Experiments in Outdoor Operation of RatSLAM", In Proc. Australasian Conference on Robotics and Automation, Canberra, Australia, pp. - , 2004.

[26] D. Scaramuzza, N. Criblez, A. Martinelli and R. Siegwart, "Robust Feature Extraction and Matching for Omnidirectional Images", In Proc. International Conference on Field and Service Robotics (FSR07), Chamonix, France, pp. 71-81, 2007.

[27] D. Scaramuzza, C. Pradalier and R. Siegwart, "Performance evaluation of a vertical line descriptor for omnidirectional images", In Proc. IEEE/RSJ International Conference on Intelligent Robots and Systems (IROS08), Nice, France, pp. 3127-3132, 2008.

[28] C. Schmid and A. Zisserman, "Automatic Line Matching Across Views", In Proc. IEEE Computer Society Conference on Computer Vision and Pattern Recognition (CVPR97), San Juan, Puerto Rico, pp. 666-671, 1997.

[29] P. Vasseur and E.M. Mouaddib, "Central catadioptric line detection", In Proc. British Machine Vision Conference (BMVC04), London, UK, pp. - , 2004.

[30] Z. Wang, F. Wu and Z. Hu, "MSLD: A robust descriptor for line matching", In Pattern Recognition (PR), Vol. 42, N5, pp. 941-953, 2009.

[31] Y. Yagi and M. Yachida, "Real-Time Generation of Environmental Map and Obstacle Avoidance Using Omnidirectional Image Sensor with Conic Mirror", In Proc. IEEE Computer Society Conference on Computer Vision and Pattern Recognition (CVPR91), Hawai, USA, pp. 160-165, 1991.

[32] X. Ying and Z. Hu,"Catadioptric line features detection using hough transform", In Proc. International Conference on Pattern Recognition (ICPR04), Cambridge, UK, pp. 839-842, 2004.

[33] Z. Zhang, "Token Tracking in a Cluttered Scene", In Image and Vision Computing (IVC), Vol. 12, N2, pp. 110-120, 1994.

[34] Z. Zhang, "Estimating Motion and Structure from Correspondences of Line Segments between Two Perspective Images", In IEEE Trans. on Pattern Analysis and Machine Intelligence (PAMI), Vol. 17, N12, pp. 1129-1139, 1995.